IJST, Transactions of Electrical Engineering, Vol. 39, No. E1, pp 93-100
Printed in The Islamic Republic of Iran, 2015

FIVE-PORT POWER SPLITTER BASED ON PILLAR PHOTONIC CRYSTAL*

M. MOHAMMADI[1**] AND M. A. MANSOURI-BIRJANDI[2]

[1]Faculty of Computer Eng., University of Payamnor Norabad Mamasani, Norabad Mamasani, Fars, I. R. of Iran
Email: masoudmohammadi23@yahoo.com
[2]Faculty of Electrical and Computer Engineering, University of Sistan and Baluchestan, Zahedan, I. R. of Iran

Abstract– Designing a power splitter with five ports has been shown in this article. In order to prevent the direct coupling between waveguides, a T-shaped structure with an appropriate distance has been used. The coupling between the parallel photonic crystal waveguides is based on multimode interference, while selecting the output efficiency is performed by setting the refractive coefficients and radius of cavities in the coupling area. The photonic crystal of the splitter has a square-shaped structure made of silicon rods with lattice constant "a", radius of $0.2a$ and linear refractive index of n=3.4. The filling factor of this structure is r/a=0.18. Characteristic curve of the power splitter has been simulated by means of finite difference time domain (FDTD) method. The present device can be used in the future photonic integrated circuits and optical network applications.

Keywords– Photonic crystal, power splitter, coupling area, finite difference time domain (FDTD)

1. INTRODUCTION

Choosing an appropriate environment for light emission with minimum power dissipation is desirable in optical devices. Photonic crystals are the novel type of optical structures that create a suitable environment for light emission [1]. The photonic crystals have become a subject of great interest during the past few years as a result of exhibiting good features [1, 2]. Photonic crystal is an environment of alternate optical properties wherein at least two materials with different dielectric constant are repeated periodically. Some stopping bands in the structures make electromagnetic wave propagation impossible. By causing a defect in the photonic crystal structures, some virtual modes within band gaps are produced that can act as a cavity resonance or waveguide [3]. Through directional coupling between two or more photonic crystal waveguides, it is possible to create power splitters, optical switches [4], polarization splitters [5, 6], mirrors [7, 8], splitters [9] and also filters [10, 11]. Among the devices mentioned above, the splitter is one of the most important components in the optical integrated circuits being used in many systems. The devices made by the photonic crystal structures have some advantages such as considerable reduction in their size compared to their counterparts, whereas as a result of this unique feature, they lead to miniaturization and integration of the optical devices in large scale. Many devices used in optical integrated circuits have been made by the photonic crystals and it is expected that they will play an important role in optical circuits as well [12, 13].

A waveguide can be created by making linear defects within a photonic crystal structure. The photonic waveguides have much smaller dimensions in comparison to the electronic waveguides; however, the power splitters are constructed by a combination of waveguides wherein the connections of

*Received by the editors January 9, 2014; Accepted May 12, 2015.
**Corresponding author

such waveguides have been proposed as T, Y junctions while the waveguide combinatory couplers have been proposed along with cavity (PCWs Coupler) [14].

Today, Y-junction structures and also high bending structures cannot be easily made due to bending losses and lack of conformity in the joints. Considering the practical design of photonic integrated circuits and the complex problems that Y branch faces has led to efforts to use the linear defect waveguides coupling properties of photonic crystals. T-junction has been used in this research because it has a smaller structure than Y-junction [15]. One way to design power splitters is to use the waveguides in combination with normal and coupled cavities [16]. The transmitted power is created by the coupling between waveguides. In other words, the transition power can be easily controlled by setting several parameters including refractive index, distance and rods radius of coupling area. An advantage in this method is the displacement change in the structure has not been used due to practical problems. Instead, the change in refractive index and rod radius in the structure has been used since they can be easily implemented.

2. STRUCTURE DESIGN

Figure 1 shows the proposed five-port power splitter structure. Due to the simple structure, integrability and little loss, the optical power splitter has been implemented through a T-shaped waveguide. In this paper, power splitter is designed using 2D square lattice photonic crystal. The number of circular rods considered for both 'X' and 'Z' directions is 61 and 41, respectively. In this structure, silicon rods with linear refractive index of n=3.4(ε_r = 11.97), radius of r=0.2a and filling factor of r/a=0.18 with square topology are located in the air substrate. This structure includes one input waveguide (P_i), five output waveguides (P_{O1}, P_{O2}…, and P_{O5}) and two coupling areas (C_1, and C2). The central waveguide is called bus waveguide whereas the output waveguides are dropping waveguide. The bus waveguide is created by removing a single line defect along ΓK direction. The coupling area of CR1 is placed between drop waveguides of 1 and 5 with the bus waveguide. Similarly, the coupling area of C_2 includes the two rows of rods in between two drop waveguides of 2 and 4 with the bus waveguide. The type of power splitter can be determined by setting radius and rods refraction coefficients in the two coupling areas (C_1 and C_2). Figure 2 depicts the first Brillouin zone of the square lattice. As sketches in Fig. 3 illustrate, a photonic band gap (PBG) is found only for the transverse magnetic (TM) polarization. The normalized frequency of TM PBG is shown from 0.445 a/λ to 0.325 a/λ whose corresponding wavelength ranges from 1213 nm to 1670 nm.

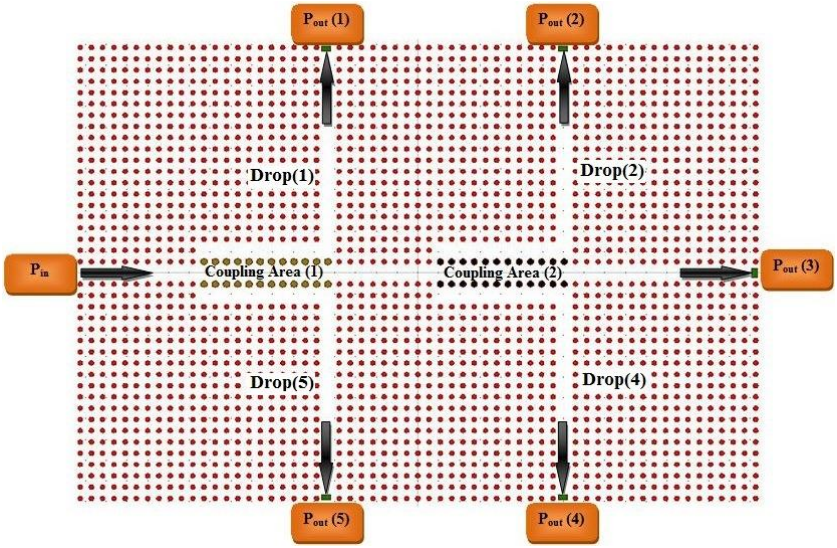

Fig. 1. Schematic diagram of the five-port power splitter using "radius change" and "refractive index change"

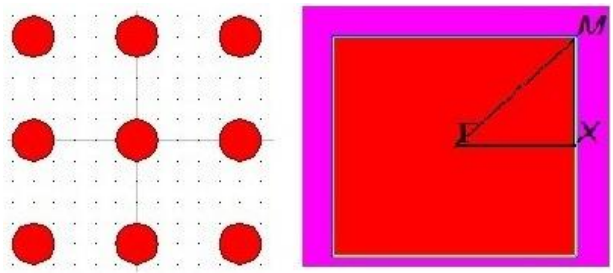

Fig. 2. A Brillouin zone of square lattice

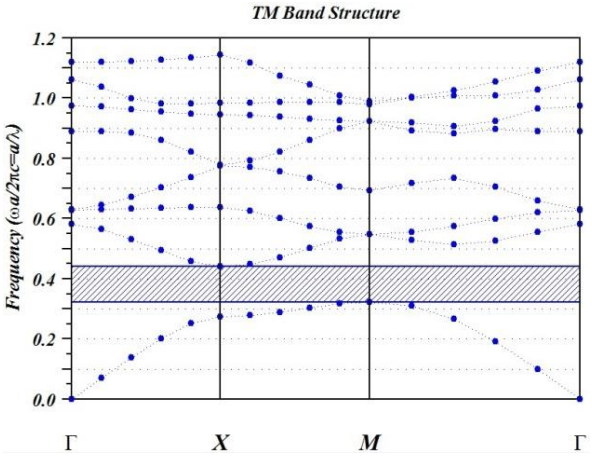

Fig. 3. Band diagram of 61×41

The coupled mode theory (CMT) has been used to study the proposed structure [16-18]. The required results can be achieved in this method by means of coupling between the cavities and bus/drop waveguides and also by setting the radius and refraction coefficients of these cavities in the coupling areas. Setting 1×1 to 1×5 splitters can be accomplished based on a similar structure. Coupling areas can be divided into three parts: a) Single-mode input waveguide b) Multi-mode coupling region c) Single-mode output waveguides.

3. POWER SPLITTER SIMULATION BASED ON RADIUS CHANGE

A Gaussian input signal is launched into the left side of bus waveguide 'Pin'. The normalized transmission spectra are calculated by 2D-FDTD method. Power monitors were placed at each of the other five ports ($P_{out}1$, $P_{out}2$, $P_{out}3$, $P_{out}4$ and $P_{out}5$) to save the transmitted spectral power density. According to Figs. 4 and 5, for a total transfer of power to the port $P_{OUT}(3)$, called 1×1 power splitter, the radius of dielectric rods in the C_1 and C_2 coupling regions should be 73 and 73 nm, respectively. In this state, Pout (1), Pout (2), Pout (4) and Pout (5) outputs values are almost zero. Determining the radius of the cavities of the coupling area 1 and 2 in the A rectangular area, the power splitter 1×1 is made in Figs. 4 and 5. In 1×2 power splitter, the output port value is almost zero in all Pout (2), Pout (3) and Pout (4), while the total power is transmitted to the Pout (1) and Pout (5) ports. In this condition, only the radius of dielectric rods which equal 93 nm at the C_1 area is determinant and the rods radius at the C_2 area has no effect on Pout (1) and Pout (5) output power. Determining the radius of the cavities of the coupling region 1 in the B rectangular area, the power splitter 1×2 is provided in Figs. 4 and 5. For a total transfer of power to $P_{out}(2)$, $P_{out}(3)$, and $P_{out}(4)$ ports, called 1×3 power splitter, the dielectric rods radius at the C_1 and C_2 regions should be 120 and 75 nm, respectively. In this state, P_{out} (1) and P_{out} (5) outputs values are almost zero. The 1×3 power splitter is constructed by changing the radius of cavities within the rectangular range C and D. Figures 4 and 5 depict the rectangular range C and D respectively. For 1×4 power splitter, where the power transmittance would be to $P_{out}(1)$, $P_{out}(2)$, $P_{out}(4)$ and $P_{out}(5)$, as before, the radius of dielectric rods at the C_1 and C_2 regions should be 120 nm and 93 nm, respectively. In this state, P_{out} (3) output is almost zero. Figures 4 and 5, the radius of the cavities of the coupling area 1 and 2 in the C and F rectangular range is determined respectively, where 1×4 power splitter is created. In 1×5 power splitter, the total power has been transmitted to P_{out} (1), P_{out} (2), P_{out} (3), P_{out} (4) and P_{out} (5) ports. To achieve this status, the radius of dielectric rods at the C_1 and C_2 regions should be 120 and 83 nm, respectively. 1×5 power splitter is made to determine the radius of the cavities of the coupling area 1 and 2 in the range of the C and E rectangular

areas. The powers for output ports (1 and 5) and output ports (2 and 4) are in good agreement with each other in Figs. 4 and 5, respectively.

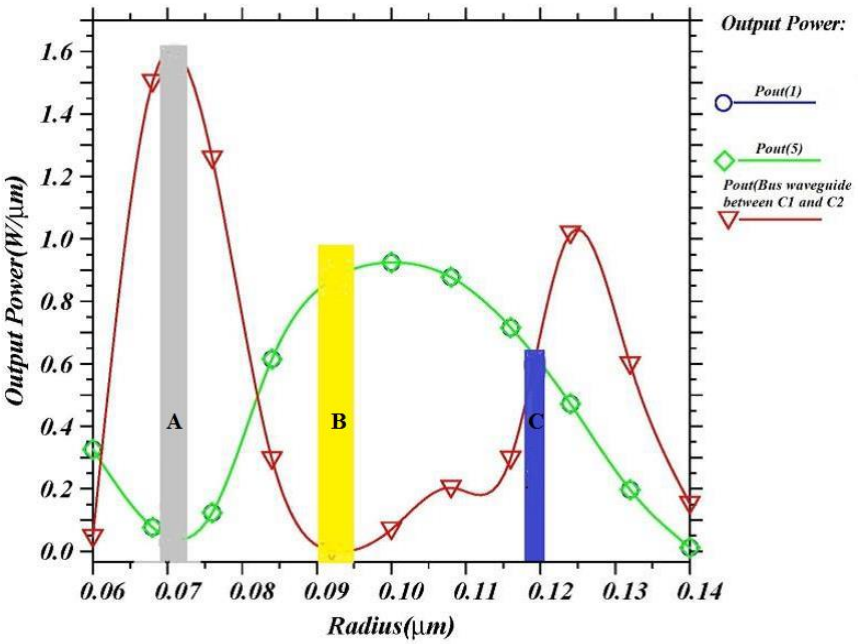

Fig. 4. Output power changes of waveguide 1, 5 and the waveguide between two coupling areas 1and 2 based on "changes in cavities radius" at the coupling area 1

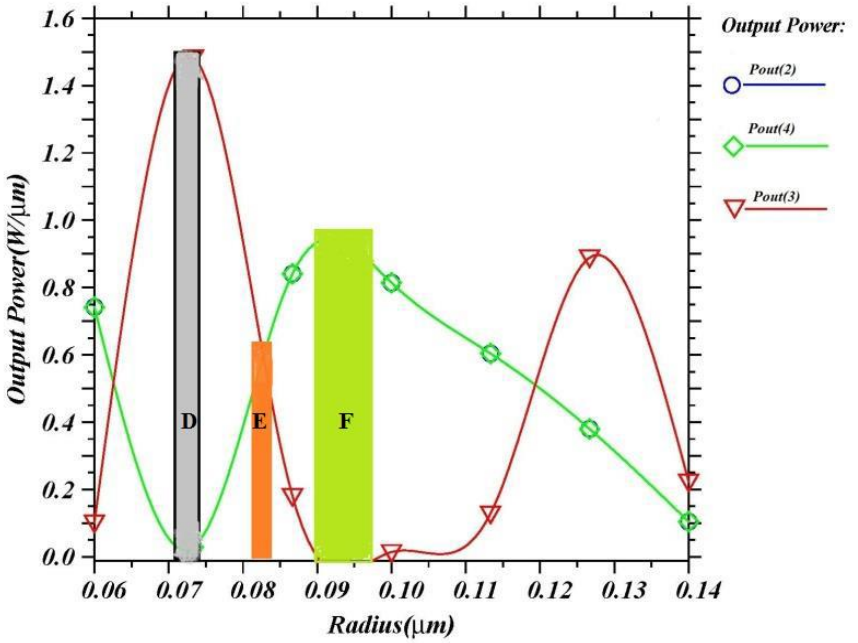

Fig. 5. Output power changes of 2, 4 and 3 waveguides based on "changes in cavities radius" at the coupling area 2

Figure 6 shows the optical field transfer curve of splitters in five different states. These five states have been created by a change made in the radius of coupling areas. To show the function of this structure as accurately as possible, the output light intensity of each port along with the defects radius values in coupling areas are given in Table 1. Figure 6a-e depicts the structure performance and electric field pattern of Power Splitter Based on Radius Change.

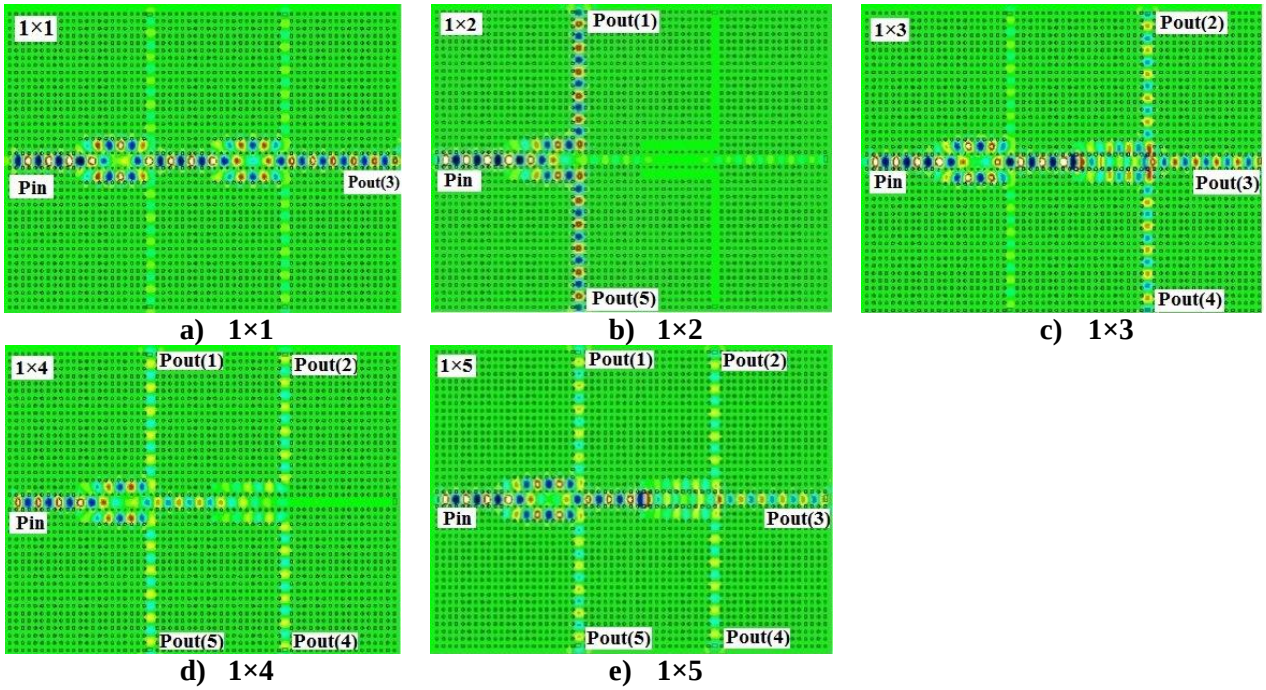

Fig. 6. Optical electric-field distribution of power splitter in five different states: a) 1×1, b) 1×2, c) 1×3, d) 1×4 and e) 1×5 by "changing the radius coefficients" at the coupling areas 1 and 2

Table 1. The results of power splitter structure design based on defects radius in coupling area 1 and 2

Type of splitter	Defects radius in coupling area 1 (μm)	Defects radius in coupling area 2 (μm)	Output Port				
			P_{O1}	P_{O2}	P_{O3}	P_{O4}	P_{O5}
1×1	0.073	0.073	0	0	1	0	0
1×2	0.093	-	1	0	0	0	1
1×3	0.120	0.075	0	1	1	1	0
1×4	0.120	0.093	1	1	0	1	1
1×5	0.120	0.083	1	1	1	1	1

4. POWER SPLITTER SIMULATION BASED ON THE CHANGE IN REFRACTIVE INDEX

The process of this splitter design based on the change in refractive index in the coupling area is now being explained. In this way, no changes have been made in the radius of rods and only by changing the refractive index of rods at the coupling areas (C_1 and C_2) can the output powers of ports be adjusted. A broadband Gaussian pulse is launched into input port, and monitors are then placed inside each bus and drop waveguide of the power splitter, measuring the time-varying electric and magnetic field. Figure 7 shows the change in output power of the Pout (1), Pout (5) and the bus waveguide between coupling area 1 and 2 based on refractive index at coupling area 1 (C_1). Output power of the Pout (2), Pout (3) and Pout (4), based on refractive index at coupling area 2 (C_2) is shown in Fig. 8. For 1×1 power splitter, where the power transmittance would be to P_{out} (3), as before, the dielectric rods refractive index at the C_1 and C_2 regions should be 1.65 and 1.1, respectively. In this state, the output power of Pout (1), Pout (2), Pout (4) and Pout (5) are almost zero. For 1×2 power splitter, the dielectric rods refractive coefficients at C_1 region should be 1.4, while the dielectric rods refractive index at C_2 region is ineffective. Determining the refractive index at coupling area 1 in the G rectangular range in Fig. 7, 1×2 power splitter is made. The output power of Pout (2), Pout (3) and Pout (4) are nearly zero. For 1×3, 1×4 and 1×5 power splitters, the dielectric rods refractive index at C_1 and C_2 regions have been obtained 2 (1.68), 2 (1.4) and 2.5 (2),

respectively. For 1×3 the output powers of Pout (2) and Pout (4) are nearly zero. For 1×4 the output power of Pout (3) is zero. By determining the refractive index at coupling area 1 and 2 (C1 and C2) in the I, Q and K rectangular area in Figs. 7 and 8, 1×3, 1×4 and 1×5 power splitters are made respectively.

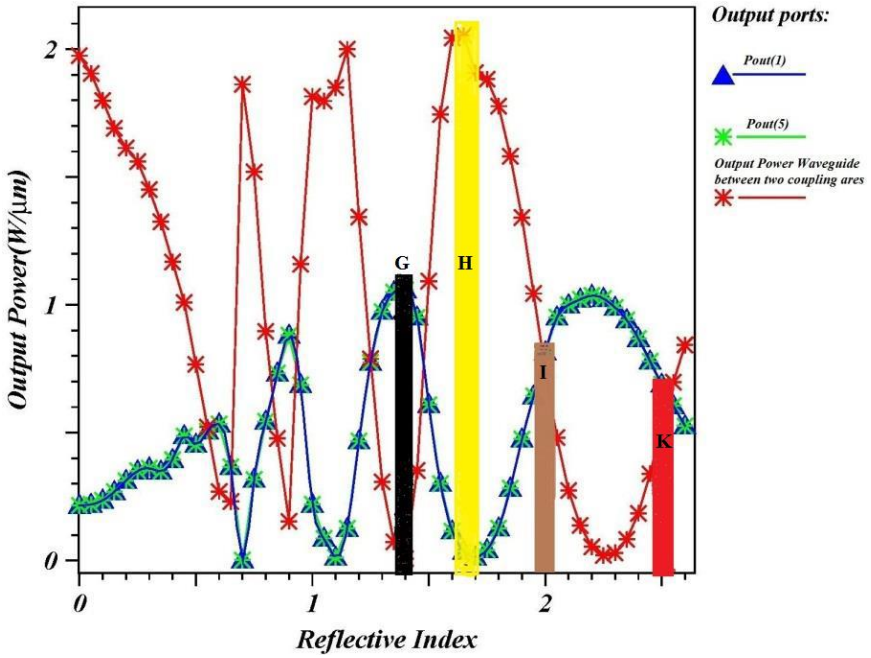

Fig. 7. Output power changes of Pout (1), Pout (5) and waveguide between two coupling area based on the "change in refractive index" at the C_1 coupling area

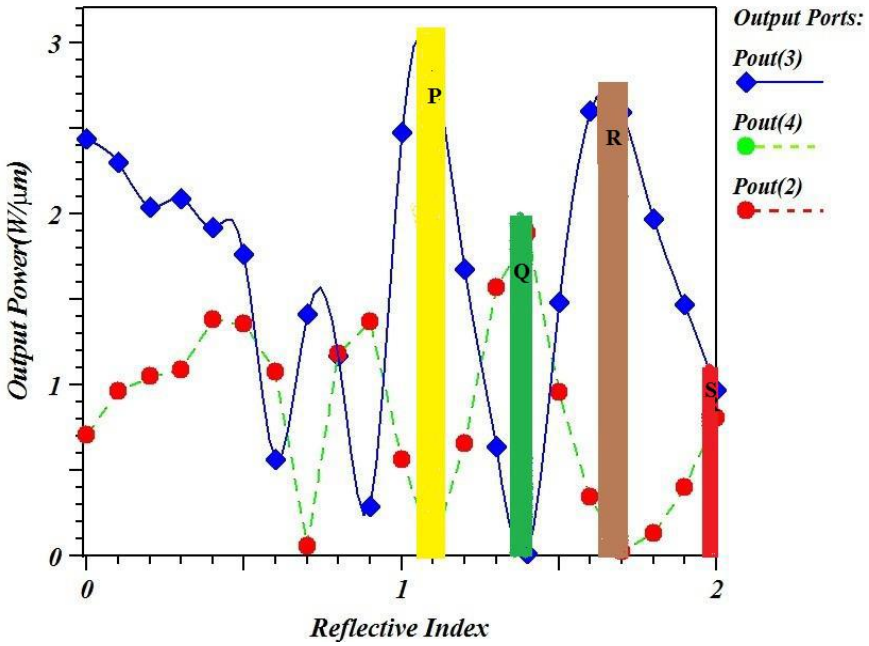

Fig. 8. Output power changes of Pout (2), Pout (3) and Pout (4) based on the "change in refractive index" at the C_2 coupling area

Figure 9a-e shows the structure performance and the electric field pattern of power splitter based on change in refractive index at C1 and C2 coupling areas. These five states have been created by the change of refractive index of coupling areas (C1 and C2). To illustrate the function of this structure as precisely as possible, the output light intensity of each port along with the values of refractive index at the coupling areas 1 and 2, are given in Table 2.

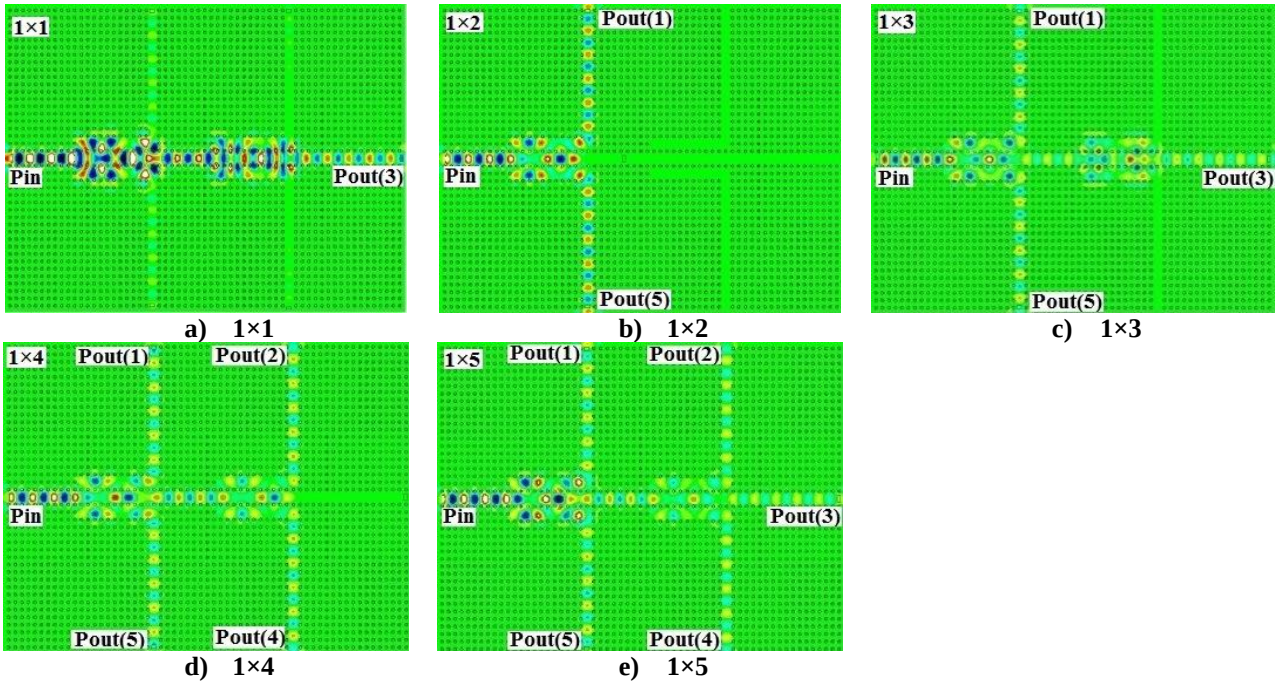

Fig. 9. Optical electric-field distribution of power splitter in five different states: a) 1×1, b) 1×2, c) 1×3, d) 1×4 and e) 1×5 by means of the "change in the refractive index" at the coupling areas 1 and 2

Table 2. The results of power splitter structure design based on the change of refractive index at the coupling areas 1and 2

Type of splitter	Change of refractive index at the coupling area 1 (n_1)	Change of refractive index at the coupling area 2 (n_2)	Output Port				
			P_{O1}	P_{O2}	P_{O3}	P_{O4}	P_{O5}
1×1	1.65	1.65	0	0	1	0	0
1×2	1.4	-	1	0	0	0	1
1×3	2	1.68	1	0	1	0	1
1×4	2	1.4	1	1	0	1	1
1×5	2.5	2	1	1	1	1	1

5. CONCLUSION

In this article, a compact integrated power splitting device with one output (1 × 1), two outputs (1× 2), three outputs (1× 3), four outputs (1 × 4) and five outputs (1× 5) channel has been designed and also simulated through coupling between waveguides, cavities and T-junction in a square structure of photonic crystal. The structure has a certain performance with optimum dimension of 61μm × 41μm. This structure includes an input waveguide, five output waveguides and two coupling areas. The photonic crystal of this structure is made of a square lattice of silicon rods with the refractive index n_1=3.46 which are perforated in air with refractive index n_2=1. In addition, using two methods "radius change" and "refractive index change" in the coupling areas, a power splitter can be designed that outputs power at each port at the desired level. The dissolution in the photonic crystal was minimized by setting the lattice constant and the radius of cavities. By using this idea, the structure can be expanded as a 1×N splitter.

REFERENCES

1. Liu, T., Zakharian, A. R. & Fallahi, M. (2004). Multimode Interference Based Photonic Crystal Waveguide Power Splitter," *Journal of Light-wave technology*, Vol. 22, No. 12, 2842-2846, 2004.

2. Foghani, Sh., Kaatuzian, H. & Danaie, M. (2010). Simulation and design of a wideband T-shaped photonic crystal splitter. *Optica Applicata*, Vol. XL, No. 4, 863-872.
3. Joannopoulos, J. D., Meade, R. D., Johnson, S. G. & Winn, J. N. (1997). Photonic crystals: Molding the Flow of Light. *Nature*, Vol. 386, pp. 143-149.
4. Mansouri-Birjandi, M. A., Moravvej-Farshi, M. K. & Rostami, A. (2008). Ultrafast low-threshold all-optical switch implemented by arrays of ring resonators coupled to a Mach–Zehnder interferometer arm: based on 2D photonic crystals. *OSA, APPLIED OPTICS*, Vol. 47, No. 27, pp. 5041-5050.
5. Li, Y. Y., Gu., P. F., Li, M. Y., Yan, H. & Liu, X. (2008). Research on the wide-angle and broadband 2D photonic crystal polarization splitter. *Journal of Electromagnetic Waves and Applications*, Vol. 20, No. 2, 265-273.
6. Shi, Y. (2010). A compact polarization beam splitter based on a multimode photonic crystal waveguide with an internal photonic crystal section. *Progress in Electromagnetics Research*, Vol. 103, pp. 393-401.
7. Manzanares-Martinez, J., Archuleta-Garcia, R., Castro-Garay, P., Moctezuma-Enriquez, D. & Urrutia-Banuelos, E. (2011). One-dimensional photonic heterostructure with broadband omnidirectional reflection. *Progress in Electromagnetics Research*, Vol. 111, pp. 105-117.
8. Wu, C. J., Hsieh, Y. C. & Hsu, H. T. (2011). Tunable photonic band gap in a doped semiconductor photonic crystal in near infrared region. *Progress in Electromagnetics Research*, Vol. 114, 271-283.
9. Dai, X. Y., Xiang, Y. & Wen, S. (2011). Broad omnidirectional reflector in the one-dimensional ternary photonic crystals containing superconductor. *Progress In Electromagnetics Research*, Vol. 120, pp. 17-34.
10. Wang, Z. Y., Cheng, X. M., He, X. Q., Fan, S. L. & Yan, W. Z. (2008). Photonic crystal narrow filters with negative refractive index structural defects. *Progress In Electromagnetics Research*, Vol. 80, pp. 421-430.
11. Hsu, H. T., Lee, M. H., Yang, T. J., Wang, Y. C. & Wu, C. J. (2011). A multichannel filter in a photonic crystal containing coupled defects. *Progress In Electromagnetics Research*, Vol. 117, PP. 379-392.
12. Park, I., Lee, H. S., Kim, H. J., Lee, S. G., Park, S. G. & Lee, E. H. (2004). Photonic Crystal Power Splitter based on directional coupling. OSA, Optical Express, Vol. 12, No.15, PP. 3598-3604.
13. Yablonovitch, (1987). Inhibited spontaneous emission in solid-state physics and electronics. *Phy. Rev. Lett*., Vol. 58, pp. 2059-2062.
14. Fan, S., Hohnson, S. G., Joannopoulos, J. D., Manolatou, C. & Haus, H. A. (2001). Waveguide branches in photonic crystals. *J. Opt. Soc. Amer. B*, Vol. 18, No. 2, pp. 162–165.
15. Yong-feng, G., Jun, Z., Ming, Z., Ming-yang, C. & Wei, Z. (2010). Design of novel power splitters by directional coupling between photonic crystal waveguides. *Optoelectronics Letters*, Vol. 6, No. 6, pp. 417-420.
16. Fasihi, K. & Mohammadnejad, S. (2009). Highly efficient channel-drop filter with a coupled cavity-based wavelength-selective reflection feedback. *OSA, Optics Express*, Vol. 17, No. 11, pp. 8983-8997.
17. Ren, H., Jiang, Ch., Hu, W., Gao, M. & Wang, J. (2006). Photonic crystal channel drop filter wit wavelength-selective reflection micro-cavity. *OSA, Optics Express*, Vol. 14, No. 6, pp. 2446-2458.
18. Li, Q., Wang, T., Su, Y., Yan, M. & Qiu, M. (2010). Coupled mode theory analysis of mode-splitting in coupled cavity system. *OSA, Optics Express*, Vol. 18, No. 8, pp. 8367-8382.